

Coherent Dark Resonances in Atomic Barium

U. Dammalapati, S. De, K. Jungmann and L. Willmann
*Kernfysisch Versneller Instituut, University of Groningen,
 Zernikelaan 25, 9747 AA Groningen, The Netherlands*

The observation of dark-resonances in the two-electron atom barium and their influence on optical cooling is reported. In heavy alkali earth atoms, i.e. barium or radium, optical cooling can be achieved using n^1S_0 - n^1P_1 transitions and optical repumping from the low lying n^1D_2 and $n^3D_{1,2}$ states to which the atoms decay with a high branching ratio. The cooling and repumping transition have a common upper state. This leads to dark resonances and hence make optical cooling less inefficient. The experimental observations can be accurately modelled by the optical Bloch equations. Comparison with experimental results allows us to extract relevant parameters for effective laser cooling of barium.

The pioneering work on optical cooling and trapping of neutral atoms as well as important advances made since then have mainly been carried out with atomic systems which have a strong optical transition connected to the ground or metastable state. Although a two-level system would be ideal, even optically rather simple accessible atoms, such as stable alkali isotopes, have hyperfine structure. This requires (re-)pumping of the atomic population into the state of highest angular momentum in order to realize an effective two-level system.

Some atoms with complex atomic structure have a unique potential for precision tests of fundamental symmetries [1, 2]. This can be exploited best with cooled and trapped atoms. Among these systems is the radium (Ra) atom, which offers a strong enhancement of a potential permanent electron Electric Dipole Moment (EDM) due to the unique close proximity of the $7s6d^3P_1$ and $7s6d^3D_2$ levels [3]. In addition it provides an excellent opportunity to find a potential nucleon EDM in some isotopes where the nuclei are octupole deformed [4]. The radioactivity of all Ra isotopes and the availability of rather small quantities requires the atoms to be cooled and trapped for experiments to achieve sufficient accuracy. Cooling and trapping of a few Ra atoms has been demonstrated recently using the $7s^2\ ^1S_0$ - $7s7p\ ^3P_1$ intercombination line [5]. The stronger $7s^2\ ^1S_0$ - $7s7p\ ^1P_1$ has a 100 times higher transition strength and therefore offers a much larger cooling force. Unfortunately for the heavy alkali earth elements barium (Ba) and Ra the branching of the decay of the excited 1P_1 state to the 1S_0 state respectively sum of the 1D_2 and the 3D states is 1:330(30) (Ba) and 1:500(80) (Ra). In the lighter alkali earth atoms Ca and Sr the ratio is 1:100000(1000) and 1:52000(500), and the transition to the 1D_2 provides the strongest of the leaks. Therefore effective repumping of the population trapped in the metastable D-states to the cooling cycle will be essential for a scheme involving the strong transition from the ground state. In addition, repumping needs to go via the same excited 1P_1 state, otherwise the atoms will be distributed over even more metastable states. We observe dark resonances, which connect the ground state and the metastable states through coherent interaction of the cooling laser and the repump lasers. These Raman

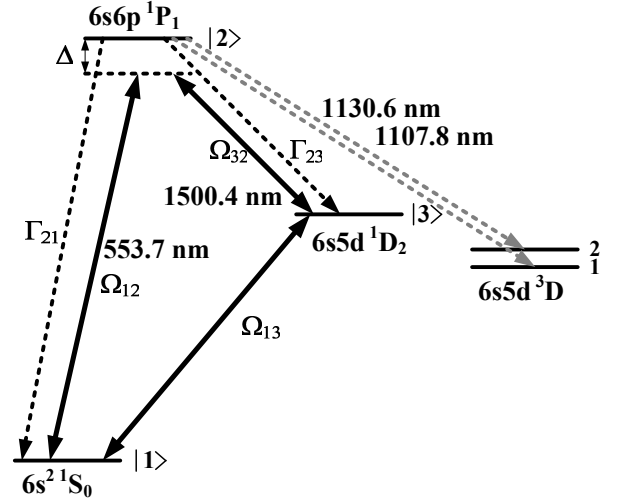


FIG. 1: Ba atomic level scheme for the observation of dark resonances. The singlet 1S_0 , 1P_1 and 1D_2 states form a "Λ - system" used here for the dark resonance measurement. They are referred to as $|1\rangle$, $|2\rangle$ and $|3\rangle$. The interaction with the coherent light fields are represented through the Rabi frequencies Ω_{12} and Ω_{32} . The decay rates Γ_{21} and Γ_{32} are given in Tab. I. A common detuning Δ for both lasers from the centers of their resonances is indicated. Other Λ-systems relevant for laser cooling with the $^3D_{1,2}$ state are also indicated.

transitions decrease the efficiency of the cooling process.

Since their first experimental observation in 1976 in sodium [6], coherent dark resonances have been observed e.g. in alkali atoms between different hyperfine states, in chromium [7] and in samarium vapor [8]. A review on the developments and status of the coherent dark state spectroscopy can be found in references [9, 10]. We have studied such processes in the heavy alkali earth atom Ba which has a number of stable isotopes and is accessible with commercial lasers for all relevant transitions. We expect that the results can be transferred directly to Ra because of the similar atomic level scheme.

The relevant part of the Ba atom energy level scheme is displayed in Fig. 1. The $6s6p\ ^1P_1$ excited state decays to the $6s^2\ ^1S_0$ ground state and weakly to the $6s5d\ ^1D_2$ metastable state. If the atom is exposed to a bichro-

matic laser field with copropagating green and infrared laser beams at $\lambda_1=553.7$ nm and $\lambda_2=1500.4$ nm, the scattered light contains a strong component λ_1 and a small component at λ_2 .

The experimental setup used to observe the coherent dark resonances in Λ -system is depicted in Fig. 2. A Ba atomic beam emerges from an oven at $T_{Ba}=800$ K. The interaction region between the atoms and the two lasers is located 60 cm downstream of the oven. The laser for the excitation of the $6s^2 \ ^1S_0 - 6s6p \ ^1P_1$ transition at $\lambda_1=553.7$ nm is a commercial Coherent 699-21 ring dye laser with Pyrromethene567 dye pumped by a Nd:YAG laser. Its linewidth is below 1 MHz. A commercial fiber laser (KOHERAS Adjustik) at $\lambda_2 = 1500.4$ nm and a linewidth of 50 kHz excites the $6s5d \ ^1D_2 - 6s6p \ ^1P_1$ transition. The two laser beams are orthogonal to the atomic beam and counter-propagated each other. They are colimated and are overlapped along the path of interaction with the atomic beam with a an angle less than 5 mrad. The beam radius of the laser at λ_2 is 1.0(0.2) mm with a Gaussian beam profile and the laser beam at λ_1 is shaped by a rectangular aperture of size 3×3 mm² to have uniform intensity distribution. The fluorescence signal from the $6s6p \ ^1P_1 - 6s^2 \ ^1S_0$ transition is detected by a photomultiplier tube with a 550 nm interference filter of 10 nm width in the axis perpendicular to both the atomic and the laser beams. The fluorescence signal is proportional to the excited 1P_1 state population.

The atom-laser interaction in this experiment is modelled as an atomic three-level Λ -system, which coherently interacts with two light fields. The formalism applied here is similar to the semi-classical scheme reported to describe the Ba ions [12, 13]. The atom is treated quantum mechanically in the Heisenberg picture and characterized by the 6 parameters $|i\rangle\langle j|$ ($i,j=1,2$ and 3). The coherent laser fields are treated as classical electromagnetic waves $\vec{E}_g \sin(\omega_g t)$ for λ_1 and $\vec{E}_r \sin(\omega_r t)$ for λ_2 . The two transitions have a linewidth Γ_g and Γ_r respectively. Spontaneous emission of photons is treated as decays from $|2\rangle$ to $|1\rangle$ and $|3\rangle$ with rates Γ_{21} and Γ_{23} .

The equations of motion for the density matrix ρ of the atom (Bloch equations) contain terms that model the coherent coupling with the external light fields by effective Rabi frequencies Ω_{12} and Ω_{32} , which denote the strength of the coupling between the atom and the electric field of the lasers.

$$\Omega_{ij} = \frac{-eE_0}{\hbar} \langle j|r|i \rangle \quad (1)$$

where e is the charge of the electron, E_0 is the electric field of the electromagnetic wave, \hbar is Planck's constant and the last term is the transition dipole matrix element between states j and i . The rotating wave approximation, which neglects the fast oscillating terms, is applied [14]. The optical Bloch equations where we use the abbreviation $\tilde{\rho}_{ij} = \rho_{ij} e^{i\Delta_{ij}t}$ is

$$\frac{d\rho_{11}}{dt} = \Gamma_{21} \rho_{22} - \frac{i}{2} \Omega_{21}^* \tilde{\rho}_{12} + c.c.$$

$$\begin{aligned} \frac{d\rho_{22}}{dt} &= -(\Gamma_{21} + \Gamma_{23}) \rho_{22} + \frac{i}{2} \Omega_{12}^* \tilde{\rho}_{21} - \frac{i}{2} \Omega_{32}^* \tilde{\rho}_{32} + c.c. \\ \frac{d\rho_{33}}{dt} &= \Gamma_{23} \rho_{22} + \frac{i}{2} \Omega_{32}^* \tilde{\rho}_{23} + c.c. \\ \frac{d\tilde{\rho}_{12}}{dt} &= -\left[\frac{\Gamma_{12} + \Gamma_{23}}{2} - i\Delta_{12}\right] \tilde{\rho}_{12} \\ &\quad + \frac{i\Omega_{12}^*}{2}(\rho_{11} - \rho_{22}) + \frac{i}{2} \Omega_{32} \tilde{\rho}_{31} \\ \frac{d\tilde{\rho}_{13}}{dt} &= -i[(\Delta_{12} - \Delta_{32})\tilde{\rho}_{13} - \frac{\Omega_{32}}{2}\rho_{23} + \frac{\Omega_{12}}{2}\tilde{\rho}_{21}] \\ \frac{d\tilde{\rho}_{23}}{dt} &= -\left[\frac{\Gamma_{12} + \Gamma_{23}}{2} - i\Delta_{23}\right] \tilde{\rho}_{23} + \frac{i}{2} \Omega_{32}(\rho_{22} - \rho_{33}) \\ &\quad - \frac{i}{2} \Omega_{12} \tilde{\rho}_{31} + \frac{i\Omega_{32}}{2}(\rho_{33} - \rho_{22}). \end{aligned} \quad (2)$$

The equations are solved numerically for our experimental conditions. In additions we take the moving of the atoms through the laser fields into account by considering the finite time the atoms spent in the respective laser beams. A Maxwell-Boltzmann velocity distribution at temperature T_{Ba} for the atoms in an atomic beam is assumed.

Depending on the detuning Δ_{32} of the laser at λ_2 from the $6s5d \ ^1D_2 - 6s6p \ ^1P_1$ transition and the detuning Δ_{12} of the laser at λ_1 from the $6s^2 \ ^1S_0 - 6s6p \ ^1P_1$ transition the atoms are driven coherently between the 1S_0 and the 1D_2 -states without passing through the 1P_1 state. For the resonance condition $\Delta = \Delta_{12} = \Delta_{32}$ and the detuning Δ much larger than the Rabi frequencies Ω_{12} and Ω_{32} the effective Rabi frequency for the Raman transition can be written as

$$\Omega_{13} = \frac{\Omega_{12} \Omega_{32}}{2\Delta}. \quad (3)$$

For an intensity of $I = 1$ mW/cm² of both lasers the estimated Rabi frequencies (Eq.1) are given in Table I together with the spontaneous transition coefficients. However, for effective cooling $\Delta_{12,32}$ are both on the order of the linewidth of the transitions and Eq. 3 is not applicable. Thus the full optical Bloch equations need to be evaluated.

The fluorescence spectrum observed shown in Fig. 3 is obtained by scanning the frequency of the laser at λ_1 in the absence of the laser at λ_2 . Contributions from different isotopes of Ba are visible. The solid line in the figure

TABLE I: Wavelengths λ_{ik} , transition probabilities A_{ik} [16, 17] and Rabi frequencies Ω_{ik} at a laser beam intensity $I = 1$ mW/cm² for the relevant transitions in Ba.

Transition	λ_{ik} [nm]	Γ_{ik} [10 ⁸ s ⁻¹]	Ω_{ik} [rad/s]
$6s^2 \ ^1S_0 - 6s6p \ ^1P_1$	553.7	1.19(1)	$22 \cdot 10^6$
$6s5d \ ^1D_2 - 6s6p \ ^1P_1$	1500.4	0.0025(2)	$4.7 \cdot 10^6$
$6s5d \ ^3D_2 - 6s6p \ ^1P_1$	1130.6	0.0011(2)	$2.0 \cdot 10^6$
$6s5d \ ^3D_1 - 6s6p \ ^1P_1$	1107.8	0.000031(5)	$0.32 \cdot 10^6$

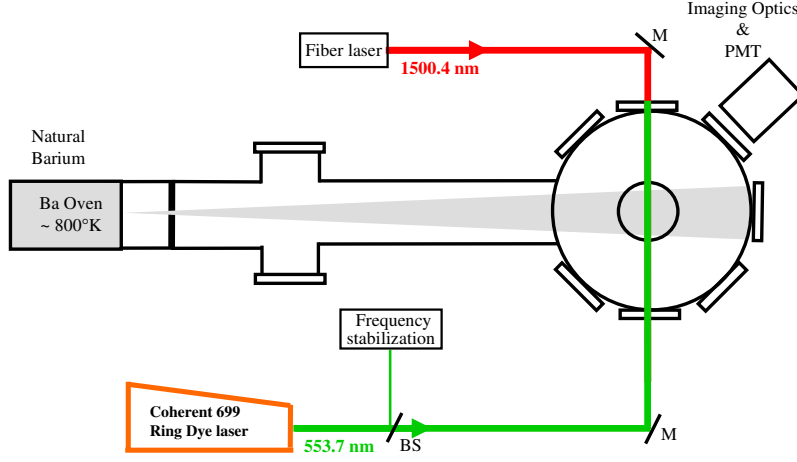


FIG. 2: A beam of atomic Ba with natural isotope composition emerges from an oven heated to ≈ 800 K. The two counter-propagating laser beams cross the atomic beam at right angle 0.6 m downstream, limiting the divergence of the atomic beam to 30 mrad. Fluorescence from the $6s6p\ ^1P_1$ state is detected with a photomultiplier tube (PMT).

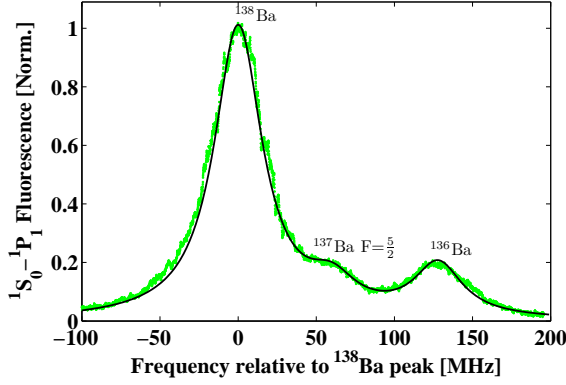


FIG. 3: Green fluorescence spectrum from the 1P_1 state detected with a beam of natural Ba in the absence of the laser at λ_2 . The experimental spectrum is well described by a numerical solution of the optical Bloch equations (solid line) when the spectra are normalized to the peak amplitude.

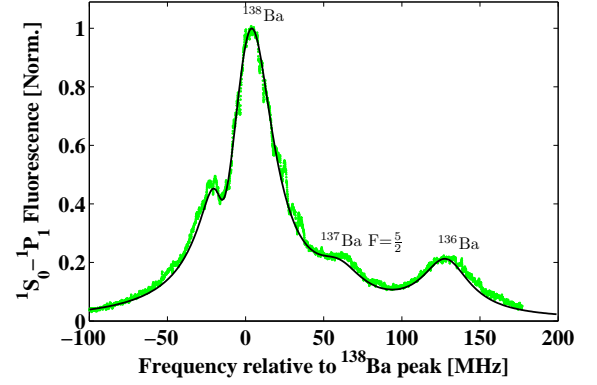


FIG. 4: Green fluorescence spectrum from the 1P_1 state detected with in beam of natural Ba. A numerical solution of the optical Bloch equation using $\Omega_{12} = 120 \cdot 10^6$ rad/s and $\Omega_{32} = 100 \cdot 10^6$ rad/s describes the experimental data well.

represents the numerical solution of Eqns. (2). The spectra are normalized to the peak amplitude of the ^{138}Ba resonance. The other isotope contributions are according to their natural abundance and their known isotope shift [15].

Fig. 4 gives the fluorescence spectrum obtained with the laser at λ_2 (red) detuned by $\Delta_2 = -13.5(5)$ MHz with respect to the center of the $6s5d\ ^1D_2 - 6s6p\ ^1P_1$ transition in the ^{138}Ba isotope. The frequency of the laser at λ_1 is scanned across the resonance. The laser power at λ_2 is 10(1) mW yielding an intensity of 320(120) mW/cm². This corresponds to a Rabi frequency $\Omega_{32} = 80(30) \cdot 10^6$ rad/s. The laser at λ_1 at a power of 2.2(1) mW, or an intensity of 24(1) mW/cm², we yield a Rabi frequency of $\Omega_{12} = 120(3) \cdot 10^6$ rad/s. The laser linewidth for the two lasers is much less than the Rabi frequencies and the decay rate of the $6s6p\ ^1P_1$

state. In the calculations a laser linewidth of $\Gamma_g = 1$ MHz at λ_1 and $\Gamma_r = 50$ kHz at λ_2 is assumed. The spectra are normalized to the peak amplitude. The only adjustable parameter is the ratio of the coherent Raman transition fraction to the regular fluorescence spectrum due to atoms not passing through both of the laser beams. The latter contributes 45(15) % to the ^{138}Ba fluorescence.

The dip on the left side of the resonance in ^{138}Ba is the two-photon Raman transition. The fluorescence is reduced because of the direct coupling of the $6s^2\ ^1S_0$ ground state and the $6s5d\ ^1D_2$ state. The solid line is the numerical solution with the parameter for detuning and the Rabi frequency given above. This demonstrates that the numerical approach fully describes the atomic response, and such a measurement can be used to extract the Rabi frequencies Ω_{12} and Ω_{32} .

We have observed the dark resonance in a second measurement. Here, the green laser at λ_1 was frequency

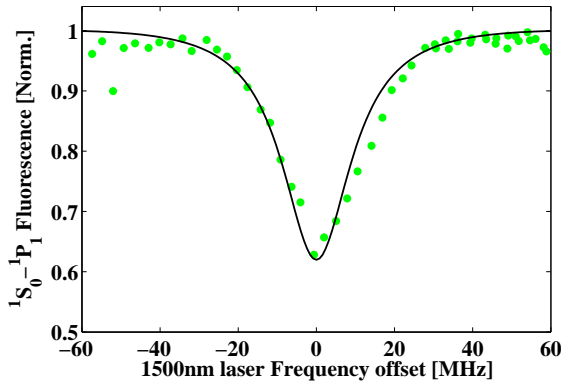


FIG. 5: The measured dark resonance spectrum for the 1P_1 state. Here the laser at $\lambda_1 = 553.7$ nm is frequency locked to resonance peak in ^{138}Ba and the laser at $\lambda_2 = 1500.4$ nm laser is scanned.

locked to the peak of the transition in the ^{138}Ba isotope using a Doppler shift method [11] and the infrared laser at λ_2 was scanned across the resonance (Fig. 5). As long as the infrared laser detuning Δ_{32} is much larger than the linewidth we observe unperturbed scattering from the $6s^2\ ^1S_0 - 6s6p\ ^1P_1$ transition. When the detuning Δ_{32} approaches the resonance the scattering rate decreases, because of coherent population transfer to the metastable $6s5d\ ^1D_2$ state. The width of the observed dip is 20(1) MHz, in good agreement with the linewidth from the numerical calculation of 19 MHz for this transition. This agreement indicates that residual Doppler broadening due to improper overlap of the laser beams was small. The solid, smooth line represents the numerical solution of the optical Bloch equations with

$\Omega_{12} = 100 \cdot 10^6 \text{ rad/s}$, $\Delta_{12} = 0$ MHz and $\Gamma_1 = 1$ MHz for the laser at λ_1 ; $\Omega_{32} = 120 \cdot 10^6 \text{ rad/s}$, and $\Gamma_2 = 50$ kHz for the laser at λ_2 . The fluorescence is normalized to the peak values and again get a good agreement between the experiment and our model.

Thus we can expect that Rabi frequencies of several 10^7 rad/s can be achieved with a laser beam diameter of 5 mm and the available laser power of 10 mW from the fiber laser. To achieve the same Rabi frequency for the $6s5d\ ^3D_2 - 6s6p\ ^1P_1$ transition the laser intensity has to be about 5 times larger and for $^3D_1 - 6s6p\ ^1P_1$ transition more than 100 times larger (Table I).

We have reported first measurements on dark resonances in atomic Ba. The observations in a three level subsystem can be well described with a model using numerical solutions of the optical Bloch equations. The accuracy of the determination is sufficient for the evaluation of the feasibility of laser cooling of barium. For a laser cooling scheme for Ba the repumping from 3D states have to be included. They will also exhibit coherent Raman transitions. The full 5-level system can be modelled with the same approach and solved numerically. In conclusion we expect that using the strong transition at λ_1 and the repumping through the same excited state can lead to a more effective cooling of heavy alkali earth atoms like Ba and Ra than the demonstrated laser cooling on the $7s^2\ ^1S_0 - 7s7p\ ^3P_1$ intercombination line in Ra [5]. This will allow for more stringent limits on permanent electric dipole moments in atomic systems.

This work was supported by the *Stichting voor Fundamenteel Onderzoek der Materie (FOM)* under programme 48 (TRIμP). One of us (U.D.) wishes to acknowledge the support through a *Ubbo Emmius* PhD student fellowship.

-
- [1] T. Akesson et al., hep-ph/0609216 (2006).
 - [2] K. Jungmann, Nucl. Phys. **A751**, 87 (2005); G.P.A. Berg, P. Dendooven, O. Dermois, M.N. Harakeh, R. Hoekstra, K. Jungmann, S. Kopecky, R. Morgenstern, A. Rogachevskiy, R. Timmermans, L. Willmann, and H.W. Wilschut, Nucl. Instr. Meth. **B 204**, 532 (2003).
 - [3] V.A. Dzuba, V.V. Flambaum, J.S.M. Ginges, and M.G. Kozlov, Phys. Rev. A, **66**, 012111 (2002).
 - [4] J. Engel, M. Bender, J. Dobaczewski, J. H. de Jesus, and P. Olbratowski, Phys. Rev. C **68**, 025501 (2003).
 - [5] J.R. Guest, N. D. Scielzo, I. Ahmad, K. Bailey, J. P. Greene, R. J. Holt, Z.-T. Lu, T. P. O'Connor, and D. H. Potterveld, Phys. Rev. Lett. **98**, 093001 (2007).
 - [6] G. Alzetta, A. Gozzini, L. Moi and G. Orriols, Nuovo Cimento **B 36**, 5 (1976).
 - [7] A. S. Bell, J. Stuhler, S. Locher, S. Hensler, J. Mlynek and T. Pfau, Europhys. Lett. **45**, 156 (1999).
 - [8] Yu. V. Vladimirova, B. A. Grishanin, V. N. Zadkov, N. N. Kolachevskii, A. V. Akimov, N. A. Kisilev and S. I. Kanorskii, J. Exp. and Theor. Phys. **96**, 629 (2003).
 - [9] R. Wynands and A. Nagel, Appl. Phys. **B 68**, 1 (1999).
 - [10] E. Arimondo, Prog. Opt., **XXXV**, 257 (1996).
 - [11] U. Dammalapati, Metastable D-state spectroscopy and laser cooling of barium, PhD thesis, University of Groningen. The Netherlands (2006).
 - [12] M. Schubert, I. Siemers, R. Blatt, W. Neuhauser and P.E. Toschek, Phys. Rev. **A52**, 2994 (1995).
 - [13] C. Raab, Interference experiments with the fluorescence light of Ba^+ ions, PhD thesis Universitat of Innsbruck, Austria (2001).
 - [14] R. Loudon, The quantum theory of light, Oxford University Press, 2nd edition (1983).
 - [15] W.A. Wijngaarden and J. Li, Can. J. Phys. **73**, 484 (1995).
 - [16] S. Niggli and M. C. E. Huber, Phys. Rev. **A35** 2908 (1987).
 - [17] A. Bizzarri and M. C. E. Huber, Phys. Rev. **A42**, 5422 (1990).